

The BODIPY-based chemosensor for fluorometric/ colorimetric dual channel detection of RDX and PA

Jianmei Gao, Xiaoxiao Chen, Shuqin Chen, Hu Meng, Yu Wang, Chunsheng Li, and Liang Feng

Anal. Chem., **Just Accepted Manuscript** • DOI: 10.1021/acs.analchem.9b02888 • Publication Date (Web): 09 Oct 2019

Downloaded from pubs.acs.org on October 13, 2019

Just Accepted

“Just Accepted” manuscripts have been peer-reviewed and accepted for publication. They are posted online prior to technical editing, formatting for publication and author proofing. The American Chemical Society provides “Just Accepted” as a service to the research community to expedite the dissemination of scientific material as soon as possible after acceptance. “Just Accepted” manuscripts appear in full in PDF format accompanied by an HTML abstract. “Just Accepted” manuscripts have been fully peer reviewed, but should not be considered the official version of record. They are citable by the Digital Object Identifier (DOI®). “Just Accepted” is an optional service offered to authors. Therefore, the “Just Accepted” Web site may not include all articles that will be published in the journal. After a manuscript is technically edited and formatted, it will be removed from the “Just Accepted” Web site and published as an ASAP article. Note that technical editing may introduce minor changes to the manuscript text and/or graphics which could affect content, and all legal disclaimers and ethical guidelines that apply to the journal pertain. ACS cannot be held responsible for errors or consequences arising from the use of information contained in these “Just Accepted” manuscripts.

The BODIPY-based chemosensor for fluorometric/colorimetric dual channel detection of RDX and PA

Jianmei Gao,^{†§} Xiaoxiao Chen,[‡] Shuqin Chen,^{†§} Hu Meng,[†] Yu Wang,[†] Chunsheng Li,[†] and Liang Feng^{†*}

[†] CAS Key Laboratory of Separation Sciences for Analytical Chemistry, Dalian Institute of Chemical Physics, Chinese Academy of Sciences, Dalian 116023, P. R. China

[‡] Key Laboratory of Radiopharmaceuticals, Ministry of Education, College of Chemistry, Beijing Normal University, Beijing 100875, P. R. China

[§] University of Chinese Academy of Sciences, Beijing 100049, P. R. China

Dedicated to the 70th anniversary of Dalian Institute of Chemical Physics, CAS

ABSTRACT: A fluorometric/colorimetric dual-channel chemosensor based on a hydrazine-substituted BODIPY probe has been successfully fabricated for the detection of RDX and PA. The chemosensor displays turn-on fluorescence behavior upon RDX with a detection limit of 85.8 nM, while showing turn-off response to PA with a detection limit of 0.44 μ M. Meanwhile, obvious color difference is observed by naked-eye after the reaction for RDX. Thus, in application, a two-to-two logic gate is constructed for potential application in explosive-sensing filed. Besides, a portable equipment is also established which realizes in-situ determination of RDX.

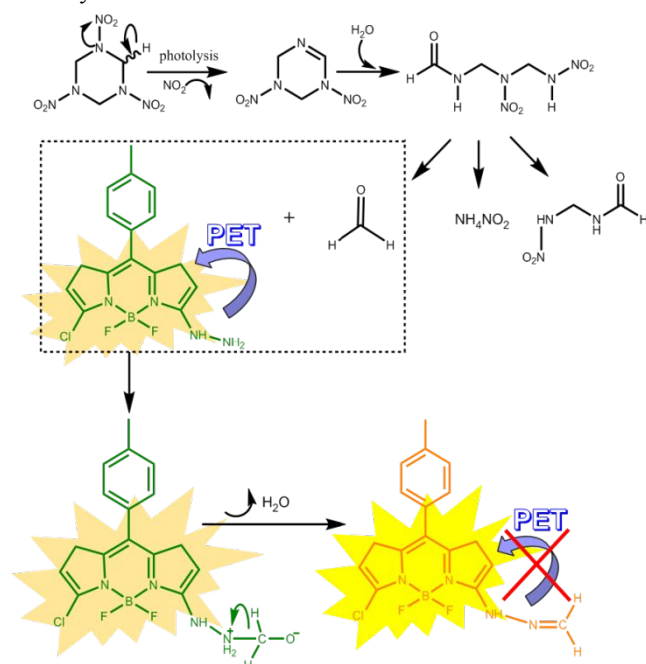
As is known to all, explosives severely endanger global security and ecological environment.^{1, 2} Among all the explosives, 1,3,5-trinitroperhydro-1,3,5-triazine (RDX) and picric acid (PA) have been widely applied in military and civilian aspects. Although the use of them is less frequent than that of 2,4,6-trinitrotoluene (TNT), the power index (PI) of these two explosives are much higher (PI_{RDX}: 127%, PI_{PA}: 100%, PI_{TNT}: 89%).³ In addition, the strong acidity and high water solubility of PA make it severely threaten the environment.^{4, 5} Thus, there is an increasing need to develop convenient and effective methods for accurate detection of RDX and PA, not only from a security perspective, but also for human health. Compared with bulky and sophisticated instrumentations, fluorescent and colorimetric chemosensors have obvious advantages such as good portability, low cost, ease of use, etc., and therefore opening up a new way for on-site detection of explosives.⁶⁻⁸

Owing to the strong electron-withdrawing groups (-NO₂) at aromatic ring, PA usually can be expediently detected by either colorimetric or fluorometric methods. Numerous optochemical sensors have been developed for PA determination based on conjugated polymers,⁹ quantum dots,^{10, 11} MOFs,^{12, 13} fluorescent molecular probes¹⁴⁻¹⁶ and silicon materials.¹⁷ However, since RDX does not have typical absorption bands derived from π - π^* or n- π^* transition, therefore, only few works have been reported to detect RDX by colorimetric means.^{18, 19} Although several fluorescent chemical sensors have been demonstrated for RDX detection, including nanofiber,²⁰ small fluorescent probes,²¹ conjugated polymers^{22, 23} and metal nanoclusters,^{24, 25} almost all these sensors show turn-off

response, which is well-known easy to be disturbed by interferences. A turn-on sensor for RDX with high sensitivity and selectivity is still highly desirable. Furthermore, to the best of our knowledge, a RDX chemosensor with the capability of detecting PA via both fluorescent and colorimetric methods has rarely been reported, which will undoubtedly more attractive.

Herein, we report a fluorescent/colorimetric dual-channel approach to detect RDX and PA based on a hydrazine-substituted BODIPY (boron-dipyrromethene) probe (named probe **1**). The strong PET effect from hydrazine to BODIPY matrix results in weak emission of probe **1** (about 0.241% compared with quinine sulfate, as given in Table S1). In the presence of HCHO, which is a major product of RDX decomposition by either alkaline hydrolysis or photolysis,^{26, 27} electrophilic addition reaction between hydrazine and HCHO takes place, leading to the formation of hydrazone (Scheme 1). Resultantly, the initial intramolecular PET pathway is shut down, and the fluorescence intensity of probe **1** is substantially increasing. By accompanied with a photolysis pretreatment, probe **1** is demonstrated capable of sensing RDX, even in the presence of most common interferents. Surprisingly, probe **1** is found undergoing inner-filter course in the presence of PA, resulting in a dramatic fluorescence quenching. Importantly, the color appearance of probe **1** only changes when RDX exists, and remains unchanged in the presence of PA. Compared with other methods, the advantage of this method is shown in Table S2. Accordingly, we develop a two-to-two logic gate to realize distinctive detection of RDX and PA based on fluorometric and colorimetric dual channel. Specifically, RDX and PA are regarded as input signals whilst the absorbance and

fluorescence intensity of probe **1** represent output signals. The four output combinations (0, 0), (1, 0), (0, 1), (1, 1) allow the direct analysis of RDX and PA. In application, we develop a handheld rapid detector for RDX, which is portable and user-friendly.



Scheme 1. Photolysis process of RDX and response to HCHO of probe **1**, which displays possible mechanism of suppression of PET.

EXPERIMENTAL METHODS

Materials and Instrumentation. RDX, PA, 2,4-dinitrotoluene (DNT) and 2,4,6-trinitrotoluene (TNT) standard solutions (1000 $\mu\text{g}/\text{mL}$) were purchased from J&K Scientific Ltd. Other reagents and solvents were of commercial quality and used without further purification. Fluorescence spectra were obtained on a HITACHI F-4600 fluorescence spectrometer. Absorption spectra were determined on a Persee TU-1901 UV-vis spectrophotometer. The pictures of the paper-based sensor were taken by a Nikon D7000 digital camera. ^1H NMR spectra were recorded on a JNM-ECZS 400M spectrometer using tetramethyl silane (TMS) as internal standard at room temperature and referenced to solvent signals. Mass spectra were obtained on a 6540 UHD Q-TOF mass spectrometer and Bruker Apex IV Fourier Transform mass spectrometer.

Theoretical Calculations. All calculations for explosives (RDX, PA, TNT, DNT) and probe **1** were carried out by the Gaussian 09 program. The structural model for corresponding explosives and probe **1** were optimized using the B3LYP/6-31G(d,p) method and the related electronic energy levels of HOMO and LUMO orbitals were also obtained by the same method.²⁸

Synthesis and Purification of probe 1. BODIPY- Cl_2 was prepared according to the reported literatures.^{29,30} BODIPY- Cl_2 (96 mg, 0.28 mmol) was dissolved in methanol, and about 10-fold hydrazine hydrate was added. After stirring in darkness at room temperature for 12 hours, the crude product was obtained via vacuum filtration (see the supporting information (SI), Scheme S1). Then, the crude product was purified by column

chromatography (dichloromethane: methanol = 60:1 as eluent) to obtain probe **1** as an orange powder (83.5 mg, 87.0 %). ^1H NMR (400 MHz, CDCl_3): δ 7.50 (s, 1H), 7.35 (d, 2H, $J = 7.7$ Hz), 7.33 (d, 2H, $J = 7.7$ Hz), 6.89 (d, 1H, $J = 4.8$ Hz), 6.59 (d, 1H, $J = 4.8$ Hz), 6.36 (d, 1H, $J = 3.8$ Hz), 6.18 (d, 1H, $J = 3.8$ Hz), 4.15 (s, 2H), 2.43 (s, 3H). ESI-MS (m/z): $[\text{M}+\text{H}]^+$ calcd. $[\text{C}_{16}\text{H}_{14}\text{BClF}_2\text{N}_4]^+$, 347.0968; found: 347.1031 (see the SI, Figure S1 and S2).

Fluorescence detection of HCHO by probe 1. 37% formaldehyde solution was diluted to different concentrations (5×10^{-6} , 1×10^{-5} , 5×10^{-5} , 1×10^{-4} , 5×10^{-4} , 7.5×10^{-4} , 1×10^{-3} , 2×10^{-3} , 4×10^{-3} , 6×10^{-3} , 8×10^{-3} , 1×10^{-2} , 2×10^{-2} , 4×10^{-2} , 6×10^{-2} , 8×10^{-2} and 0.1 M). 10 μL various concentrations of formaldehyde solution were added to 990 μL solution of probe **1** (0.5 mg probe **1** dissolved in 20 mL 80% acetonitrile, acetonitrile: $\text{H}_2\text{O} = 8:2$ (V: V)). After incubation for 10 minutes, fluorescence spectra were measured under 365 nm excitation at room temperature.

Fluorescence detection of RDX and PA by probe 1. RDX and PA standard solutions were dried under the flow of N_2 , and then were redissolved in 80% acetonitrile to various concentrations from 0 to 4×10^{-3} M. After that, 10 μL solutions were put in centrifuge tubes and irradiated by 254 nm UV lamp for 10 minutes. 990 μL of probe **1** in 80% acetonitrile solution was added to the photolytic solutions. The mixtures were left for 10 minutes' standing. Finally, the fluorescence emission spectra of products were recorded under 365 nm excitation at room temperature.

Fabrication of paper-based sensor. RDX, PA, TNT, DNT, and HCl were chosen to test fluorescent paper-based sensor. Firstly, 2 μL solution of probe **1** (0.5 mg probe **1** dissolved in 20 mL 80% acetonitrile) was dropped onto wax-printed filter paper. After the paper was dried in open air, 1 μL different analyte solution (photolysis was required for analytes) was added to the paper. The concentrations of all analytes were 40 μM , and 80% acetonitrile solution was set as blank. After drying at room temperature for a few minutes, the pictures of color spots were taken by camera, and the RGB values as well as brightness of color spots were extracted by Photoshop software.

RESULTS AND DISCUSSION

Design and Synthesis of probe 1. BODIPY derivatives are excellent candidates as an important class of optical sensors due to their high molar absorption coefficients and fluorescence quantum yields as well as good chemical stability.³¹⁻³³ Thus, we chose BODIPY as parent molecule, and employed a simple one-step nucleophilic substitution reaction to introduce hydrazine group and obtain probe **1**. The hydrazine group anchored, on the one hand, opened up a new intramolecular PET pathway to BODIPY matrix, and dramatically decreased the fluorescent intensity of intrinsic molecule. On the other hand, it endowed as-synthesized molecule with a reactive site for electrophilic reagent HCHO. The formation of hydrazine was thoroughly characterized by GC-MS and ^1H -NMR (see Figure S3 and S4). Upon the addition of HCHO, under the 365 nm UV excitation, the initial pale yellow-green fluorescence of probe **1** clearly turned to bright yellow (Figure 1a), along with a distinctive color change from yellow to orange (Figure 1b). Literarily, RDX can be decomposed by either alkaline hydrolysis or photolysis,^{26,27} and concomitantly yielded HCHO as major degradation product. As such, using probe **1** as a novel RDX

sensor seemed applicable if a suitable UV-assisted pre-treatment process was involved. Moreover, the unique excitation spectrum of probe **1** was overlapped with absorption of PA, as a result, the determination of PA was possible based

on inner-filter effect. These structural features largely guaranteed the capability of probe **1** in the detection of RDX and PA.

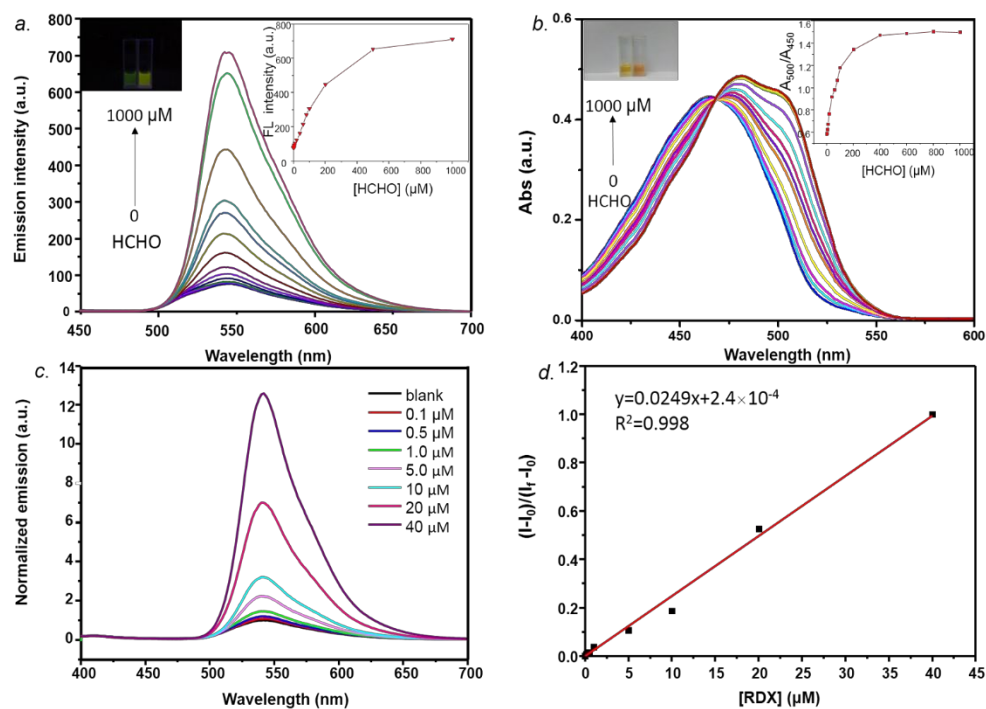


Figure 1. (a) FL emission spectra of products after interaction of probe **1** and HCHO in 80% acetonitrile, $\lambda_{ex}=365$ nm and $\lambda_{em}=540$ nm. Insets show the pictures of in the absence and presence of HCHO under 365nm UV lamp (left), as well as the fluorescence titration fitting curve (right). (b) UV-vis absorption spectra of products after interaction of probe **1** and HCHO in 80% acetonitrile. Inset shows the color change before and after interaction with HCHO in daylight (left), as well as the colorimetric titration fitting curve (right). (c) Normalized emission spectra of products after interaction of probe **1** and photolytic RDX under 254nm UV lamp. $\lambda_{ex}=365$ nm and $\lambda_{em}=540$ nm. (d) Linear relationship between growth rate of fluorescence intensity and concentrations of RDX.

The detection of RDX in dual channel. Firstly, the sensitivity of probe **1** towards RDX was determined. RDX sample was irradiated by 254 nm UV lamp for several minutes, then probe **1** was added immediately. As expected, the fluorescence intensity of probe **1** sharply increased within 3 minutes. In order to evaluate optimal irradiation time, time-resolved control trails were carried out. As shown in Figure S5, a dramatic enhancement of fluorescence intensity within 10 minutes could be observed. However, further extension of irradiation time only gave rise to a negligible enhancement of fluorescent intensity, and thus 10 minutes was chosen for pre-irradiation time ultimately. In titration experiment, by adding photolytic RDX at different concentrations, the fluorescent intensity of probe **1** gradually increased (Figure 1c). By calculation, there was a good linear regression between growth rate of fluorescent intensity and concentrations of RDX with superior regression coefficient ($R^2=0.998$) in the range of 0 to 40 μM (Figure 1d), and the limit of detection (LOD) was calculated as low as 85.8 nM based on $3\sigma/k$, where σ is relative standard deviation of blank samples, and k represents slope of standard curve, demonstrating the high sensitivity of probe **1** towards RDX. The colorimetric response of probe **1** to photolytic RDX samples was determined as well. The absorption spectrum of mixture containing probe **1** and 40 μM RDX was almost the same as that of probe **1** and HCHO mixture (see Figure S6), which further

confirmed that the detection of RDX by probe **1** shared the same mechanism as that of HCHO. This result demonstrated that probe **1** was capable of detecting RDX by both fluorometric and colorimetric method.

The selectivity and the detection of PA. In order to demonstrate the specific selectivity of probe **1** towards RDX, we firstly evaluated the interferences from common solvent and metal cations, as shown in Figure S7 and S8. All experimental procedures were the same as those adopted in RDX detection including pre-photolysis of analytes. It was clear that negligible change in fluorescence intensity was observed in all samples, elucidating the excellent working capability of probe **1**. Then, three explosives were used for further determination, including DNT, PA, TNT. Upon addition of 40 μM different explosives to probe **1**, only RDX rendered the fluorescence enhancement to probe **1**, together with an obvious color change (see Figure 2a), indicating the excellent selectivity of probe **1** towards RDX. Interestingly, the addition of PA prominently impaired the fluorescence intensity of probe **1** (see Figure 2b), quenching efficiency in presence of 40 μM PA is calculated to be 65.14%. However, the fluorescence quenching induced by PA did not reflect its color, indicating probe **1** underwent a totally different sensing mechanism in the presence of PA. By performance of PA titration experiment, the fluorescence intensity of probe **1** declined linearly as the concentration of PA increased from 0 to 40 μM , and the LOD ($3\sigma/k$) for PA was calculated as 0.44 μM

(see Figure S9 and S10). Besides, the distinguishing detection of RDX and PA could be similarly realized by probe **1**-deposited paper-based analytical device, whose feasibility was certified by principal component analysis (PCA) (see Figure S11).

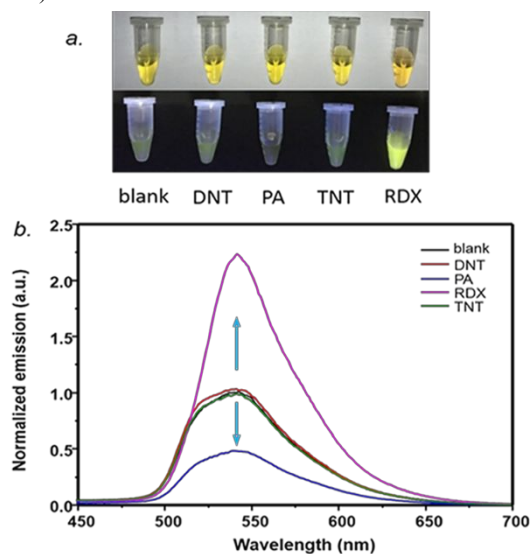


Figure 2. (a) Images of products after reaction of different explosives with probe **1** in daylight (top) and under 365 nm UV lamp (bottom). (b) Normalized emission spectra towards different explosives, the concentration of explosives is 40 Mm, $\lambda_{ex} = 365$ nm and $\lambda_{em} = 540$ nm.

Reaction Mechanism. In order to understand sensing mechanism of probe **1** towards RDX and PA, we designed several control trials. Firstly, we used H_2O_2 and $K_2S_2O_8$ to exclude oxidation effect by thin layer chromatography (TLC) method. An emissive product with the same R_f value presented in HCHO and RDX groups, as lined in red cycle in Figure S12, whereas this product was rarely observed in other groups. It distinctly proved that oxidation effect did not participate in sensing mechanism. Secondly, pH experiment was conducted to exclude the effect of alkylamines generated during photolysis process.²⁶ As the solution's pH value increased from 4 to 9 adjusted by HCl and NaOH, emission intensity of probe **1** at 520 nm rapidly increased the same as addition of different alkylamines (see Figure S13 and S14). This result was very different from those $\lambda_{em,max}$ obtained by HCHO or RDX at 540 nm, indicating that FL intensity enhancement at 540 nm was attributed to HCHO rather than alkylamines. As it has been reported that NO_2^- was a by-product as well.²⁶ With regard to this, we further employed $NaNO_2$ to exclude reactivity of probe **1** towards NO_2^- . Upon addition of 40 μM NO_2^- to reaction system, fluorescent intensity was unchanged (see Figure S15). Accordingly, the electrophilic addition reaction at hydrazine moiety by HCHO produced by photolysis of RDX seemed like the only answer left for sensing mechanism of RDX.

The fluorescence quenching mechanism of probe **1** to PA, was initially assumed originating from strong acidity of PA. However, the pH experiment controlled by HCl unambiguously elucidated that the protonation of probe **1** had almost no effect for FL intensity (as shown in Figure S16). Next, FRET behavior between PA and probe **1** was also investigated by UV-vis absorption and fluorescence emission (see Figure S17). It could be clearly seen that there was almost no overlap between absorption of PA and emission of probe **1**, which indicated that

effective FRET could hardly occur. Then, we utilized theoretical simulations to obtain the highest occupied molecular orbital (HOMO) and lowest unoccupied molecular orbital (LUMO) of probe **1**, RDX, PA, TNT, DNT.²⁸ The LUMO ($E_{LUMO} = -1.50$ eV) level of probe **1** was higher than that of all explosives (see Figure S18). That is, if electron transfer process could happen from LUMO of probe **1** to LUMO of PA, the same process should have occurred for other explosives, but we did not find the same results from TNT or DNT, so electron transfer was not the key reason for decline of emission intensity. Finally, we tested above explosives' UV-vis absorptions and probe **1**'s excitation as well as emission spectrum, which showed apparent overlap between excitation spectrum of probe **1** and absorption of PA (see Figure S19). Differently, the absorption spectra of TNT, DNT and RDX did not overlap with the excitation spectrum of probe **1**. Thus, inner-filter effect of fluorescence was considered to be a vital factor for fluorescence quenching of PA.

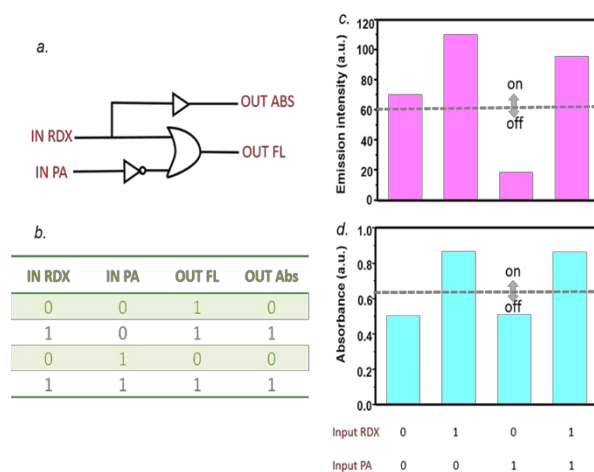


Figure 3. (a) The logic device composed of two inputs (RDX and PA) and two outputs (ABS and FL). (b) The truth table for the two-to-two decoder logic gate. (c) The column bars of emission intensity of the logic gate with a threshold of 60. (d) The column bars of absorbance of the logic gate with a threshold of 0.62.

Application. Based on the above results, we assumed that probe **1** may serve explosives' detection as a peculiar sensing platform by fluorometric and colorimetric dual detection channel. To prove this assumption, we designed a two-to-two logic gate based on optical response of probe **1** towards RDX and PA. Specifically, the two-to-two decoder converted two input bits into two output bits.³⁴ Wherein, the presence and absence of RDX (or PA) were defined as "1" and "0" of inputs, respectively, and the FL intensity at 540 nm and absorbance at 500 nm of probe **1** acted as two outputs. The threshold value was set as 60 for FL intensity and 0.62 for absorbance. Once beyond critical value, "1" signal output, otherwise "0" signal output. The logic device was illustrated in Figure 3a, the truth table together with the signal bar chart of FL intensity and absorbance of the two-to-two decoder logic gate were presented in Figure 3b, 3c and 3d. Only the presence of RDX gave rise to the signal "1" in colorimetric channel due to the uniqueness of prominent colorimetric response of probe **1** towards RDX, even in the co-existence of PA. In fluorometric channel, PA played a key role instead, which induced obvious fluorescence quenching and resulted in the output of "0" signal when there

was no RDX. The fluorescent intensity of probe **1** at 540 nm could form a logic gate combining NOT and OR to obtain IMP gate,³⁵ while absorbance at 500 nm acted as a YES gate.

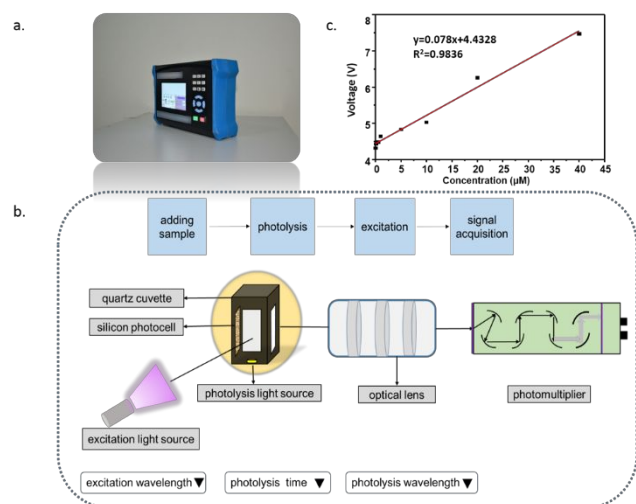


Figure 4. (a) The appearance of equipment established for RDX. (b) Schematic diagram of the equipment. (c) Standard curve obtained by the equipment.

For practical application, we developed a handheld rapid detector for fluorescent detection of RDX, as shown in Figure 4a. The detector was composed of photolysis light source (265 nm), excitation light source (365 nm), cuvette, convex lenses, optical filter and photomultiplier (Figure 4b). The size and interior circuit was demonstrated in Figure S20. In use, 20 μL liquid sample was dissolved in 80% acetonitrile aqueous solution and photolyzed for 10 minutes. 1980 μL solution of probe **1** was then mixed with RDX, and the fluorescent intensity was measured after 10 seconds. The linear regression between fluorescent intensity and concentration of RDX was illustrated in Figure 4c, which exhibited a good linearity with a considerable regression coefficient ($R^2=0.98$). This device is portable and user-friendly, providing high potential in practical detection of RDX. (For more details please see the SI, Figure S21.)

These results elucidated probe **1** possessed high potential in the distinctive detection of RDX and PA.

CONCLUSION

In summary, we have developed a facile strategy for the determination of RDX and PA using a hydrazine-substituted BODIPY probe (probe **1**) via colorimetric/fluorometric dual channel. After reacting with probe **1**, RDX and PA caused a turn-on and turn-off response in FL intensity respectively, together with color change after the reaction for RDX. Taken together, a two-to-two logic gate was constructed, which may emerge as promising candidate in explosives detection aspect. Furthermore, a portable equipment was established, indicating high potential in practical use for detection of RDX.

ASSOCIATED CONTENT

Supporting Information

The Supporting Information is available free of charge on the ACS Publications website.

Synthetic procedure of probe **1**, characterizations of probe **1** and products, fluorescence spectra and UV-Vis spectra of corresponding products, paper-based sensor, theoretical calculations of explosives, operation procedure of the portable equipment, and other supporting figures and tables.

AUTHOR INFORMATION

Corresponding Author

* E-mail: fengl@dicp.ac.cn

Notes

The authors declare no competing financial interests.

ACKNOWLEDGMENT

We are grateful for financial support from the STS project (grant no. KFJ-STC-SCYD-207) from CAS and the National Natural Science Foundation of China (Grant 21804132).

REFERENCES

- (1) Mosca, L.; Karimi Behzad, S.; Anzenbacher, P., Jr. Small-Molecule Turn-On Fluorescent Probes for RDX. *J. Am. Chem. Soc.* **2015**, *137* (25), 7967-7969.
- (2) Peng, Y.; Zhang, A. J.; Dong, M.; Wang, Y. W. A colorimetric and fluorescent chemosensor for the detection of an explosive-2,4,6-trinitrophenol (TNP). *Chem. Commun.* **2011**, *47* (15), 4505-4507.
- (3) Türker, L.; Variş, S. Structurally modified RDX - A DFT study. *Defence Technology* **2017**, *13* (6), 385-391.
- (4) Dinda, D.; Gupta, A.; Shaw, B. K.; Sadhu, S.; Saha, S. K. Highly selective detection of trinitrophenol by luminescent functionalized reduced graphene oxide through FRET mechanism. *ACS Appl. Mater. Interfaces* **2014**, *6* (13), 10722-10728.
- (5) Kaur, S.; Bhalla, V.; Vij, V.; Kumar, M. Fluorescent aggregates of hetero-oligophenylene derivative as "no quenching" probe for detection of picric acid at femtogram level. *J. Mater. Chem. C* **2014**, *2* (20), 3936-3941.
- (6) Jiang, Y.; Zhao, H.; Zhu, N.; Lin, Y.; Yu, P.; Mao, L. A simple assay for direct colorimetric visualization of trinitrotoluene at picomolar levels using gold nanoparticles. *Angew. Chem. Int. Ed.* **2008**, *47* (45), 8601-8604.
- (7) Huang, J.; Gu, J.; Meng, Z.; Jia, X.; Xi, K. Signal enhancement of sensing nitroaromatics based on highly sensitive polymer dots. *Nanoscale* **2015**, *7* (37), 15413-20.
- (8) Dong, M.; Wang, Y. W.; Zhang, A. J.; Peng, Y. Colorimetric and fluorescent chemosensors for the detection of 2,4,6-trinitrophenol and investigation of their co-crystal structures. *Chem-Asian J.* **2013**, *8* (6), 1321-1330.
- (9) Del Rosso, P. G.; Romagnoli, M. J.; Almassio, M. F.; Barbero, C. A.; Garay, R. O. Diphenylanthrylene and diphenylfluorene-based segmented conjugated polymer films as fluorescent chemosensors for nitroaromatics in aqueous solution. *Sens. Actuators, B* **2014**, *203*, 612-620.
- (10) Dutta, P.; Saikia, D.; Adhikary, N. C.; Sarma, N. S. Macromolecular Systems with MSA-Capped CdTe and CdTe/ZnS Core/Shell Quantum Dots as Superselective and Ultrasensitive Optical Sensors for Picric Acid Explosive. *ACS Appl. Mater. Interfaces* **2015**, *7* (44), 24778-24790.
- (11) Lin, L.; Rong, M.; Lu, S.; Song, X.; Zhong, Y.; Yan, J.; Wang, Y.; Chen, X. A facile synthesis of highly luminescent nitrogen-doped graphene quantum dots for the detection of 2,4,6-trinitrophenol in aqueous solution. *Nanoscale* **2015**, *7* (5), 1872-1878.
- (12) Yingli Hu; Meili Ding; Xiao-Qin Liu; Lin-Bing Sun; Jiang, H.-L. Rational synthesis of an exceptionally stable Zn(II) metal-organic framework for the highly selective and sensitive detection of picric acid. *Chem. Commun.* **2016**, *52*, 5734-5737.

- (13) Gao, Y.; Qi, Y.; Zhao, K.; Wen, Q.; Shen, J.; Qiu, L.; Mou, W. An optical sensing platform for the dual channel detection of picric acid: The combination of rhodamine and metal-organic frameworks. *Sens. Actuators, B* **2018**, *257*, 553-560.
- (14) Yogesh Erande; Santosh Chemate; Ankush More; Sekar, N. PET governed fluorescence "Turn ON" BODIPY probe for selective detection of picric acid. *RSC Adv.* **2015**, *5*, 89482-89487.
- (15) Pandith, A.; Kumar, A.; Lee, J.-Y.; Kim, H.-S. 9-Anthracenecarboxamide fluorescent probes for selective discrimination of picric acid from mono- and di-nitrophenols in ethanol. *Tetrahedron Lett.* **2015**, *56* (51), 7094-7099.
- (16) Govindasamy Sathiyar; Sakthivel, P. A multibranch carbazole linked triazine based fluorescent molecule for the selective detection of picric acid. *RSC Adv.* **2016**, *6*, 106705-106715.
- (17) Han, Y.; Chen, Y.; Feng, J.; Liu, J.; Ma, S.; Chen, X. One-Pot Synthesis of Fluorescent Silicon Nanoparticles for Sensitive and Selective Determination of 2,4,6-Trinitrophenol in Aqueous Solution. *Anal. Chem.* **2017**, *89* (5), 3001-3008.
- (18) He, Y.; Wang, L. Base-driven sunlight oxidation of silver nanoparticles for label-free visual colorimetric detection of hexahydro-1,3,5-trinitro-1,3,5-triazine explosive. *J. Hazard. Mater.* **2017**, *329*, 249-254.
- (19) Uzer, A.; Can, Z.; Akin, I.; Ercag, E.; Apak, R. 4-Aminothiophenol functionalized gold nanoparticle-based colorimetric sensor for the determination of nitramine energetic materials. *Anal. Chem.* **2014**, *86* (1), 351-356.
- (20) Xiong, W.; Liu, X.; Wang, T.; Zhang, Y.; Che, Y.; Zhao, J. Fluorescence Detection of a Broad Class of Explosives with One Zinc(II)-Coordination Nanofiber. *Anal. Chem.* **2016**, *88* (22), 10826-10830.
- (21) Wang, C.; Huang, H.; Bunes, B. R.; Wu, N.; Xu, M.; Yang, X.; Yu, L.; Zang, L. Trace Detection of RDX, HMX and PETN Explosives Using a Fluorescence Spot Sensor. *Sci. Rep.* **2016**, *6*, 25015-25023.
- (22) Gopalakrishnan, D.; Dichtel, W. R. Direct detection of RDX vapor using a conjugated polymer network. *J. Am. Chem. Soc.* **2013**, *135* (22), 8357-8362.
- (23) Gopalakrishnan, D.; Dichtel, W. R. Real-Time, Ultrasensitive Detection of RDX Vapors Using Conjugated Network Polymer Thin Films. *Chem. Mater.* **2015**, *27* (11), 3813-3816.
- (24) Enkin, N.; Sharon, E.; Golub, E.; Willner, I. Ag nanocluster/DNA hybrids: functional modules for the detection of nitroaromatic and RDX explosives. *Nano. Lett.* **2014**, *14* (8), 4918-4922.
- (25) Essner, J. B.; Chen, X.; Wood, T. D.; Baker, G. A. Tandem copper and gold nanoclusters for two-color ratiometric explosives detection. *Analyst* **2018**, *143* (5), 1036-1041.
- (26) Vimal K. Balakrishnan; Annamariahalasz; Jalal Hawari. Alkaline Hydrolysis of the Cyclic Nitramine Explosives RDX, HMX, and CL-20: New Insights into Degradation Pathways Obtained by the Observation of Novel Intermediates. *Environ. Sci. Technol.* **2003**, *37*, 1838-1843.
- (27) J. Hawari; A. Halasz; C. Groom; S. Deschamps; L. Paquet; C. Beaulieu; A. Corriveau, Photodegradation of RDX in Aqueous Solution: A Mechanistic Probe for Biodegradation with Rhodococcus sp. *Environ. Sci. Technol.* **2002**, *36*, 5117-5123.
- (28) Ju, B.; Wang, Y.; Zhang, Y. M.; Zhang, T.; Liu, Z.; Li, M.; Xiao-An Zhang, S. Photostable and Low-Toxic Yellow-Green Carbon Dots for Highly Selective Detection of Explosive 2,4,6-Trinitrophenol Based on the Dual Electron Transfer Mechanism. *ACS Appl. Mater. Interfaces* **2018**, *10* (15), 13040-13047.
- (29) Mukulesh Baruah; Wenwu Qin, N. B.; Wim M. De Borggraeve; Boens, N. I. BODIPY-Based Hydroxyaryl Derivatives as Fluorescent pH Probes. *J. Org. Chem.* **2005**, *70*, 4152-4157.
- (30) Dylan W. Domaille; Li Zeng; Chang, C. J., Visualizing Ascorbate-Triggered Release of Labile Copper within Living Cells using a Ratiometric Fluorescent Sensor. *J. Am. Chem. Soc.* **2010**, *132*, 1194-1195.
- (31) Kobayashi, T.; Komatsu, T.; Kamiya, M.; Campos, C.; Gonzalez-Gaitan, M.; Terai, T.; Hanaoka, K.; Nagano, T.; Urano, Y. Highly activatable and environment-insensitive optical highlighters for selective spatiotemporal imaging of target proteins. *J. Am. Chem. Soc.* **2012**, *134* (27), 11153-11160.
- (32) Ulrich, G.; Ziessel, R.; Harriman, A. The chemistry of fluorescent bodipy dyes: versatility unsurpassed. *Angew. Chem. Int. Ed.* **2008**, *47* (7), 1184-1201.
- (33) Jia, M. Y.; Niu, L. Y.; Zhang, Y.; Yang, Q. Z.; Tung, C. H.; Guan, Y. F.; Feng, L., BODIPY-based fluorometric sensor for the simultaneous determination of Cys, Hcy, and GSH in human serum. *ACS Appl. Mater. Interfaces* **2015**, *7* (10), 5907-5914.
- (34) Xu, X. Y.; Lian, X.; Hao, J. N.; Zhang, C.; Yan, B., A Double-Stimuli-Responsive Fluorescent Center for Monitoring of Food Spoilage based on Dye Covalently Modified EuMOFs: From Sensory Hydrogels to Logic Devices. *Adv Mater* **2017**, *29* (37).
- (35) Liu, J.; He, X.; Zhang, J.; He, T.; Huang, L.; Shen, J.; Li, D.; Qiu, H.; Yin, S. A BODIPY derivative for colorimetric and fluorometric sensing of fluoride ion and its logic gates behavior. *Sens. Actuators, B* **2015**, *208*, 538-545.

Insert Table of Contents artwork here

